JOURNAL OF MOLECULAR SPECTROSCOPY **158,** 177–200 (1993)

The Visible Absorption Spectrum of Matrix-Isolated NH_2 and Its Deuterides—Comparison with Calculated Spectroscopic Properties

CARSTEN BLINDAUER, MILJENKO PERIĆ,[1] AND U. SCHURATH

Institut für Physikalische und Theoretische Chemie der Universität Bonn, Wegelerstrasse 12, D-5300 Bonn 1, Germany

Absorption spectra of matrix-isolated NH_2 and its deuterides were measured in the range 370–880 nm. Comparison with calculated term values, transition moments, spin–orbit splittings, and with gas-phase data rendered possible the nearly complete assignment of the spectra. At 5 K the $\tilde{A}\,^2A_1, \tilde{X}\,^2B_1\,(v_1, v_2, 0) \leftarrow \tilde{X}\,^2B_1\,(0, 0, 0)$ system consists of Π-bands, and of very weak $\Sigma^* \leftarrow \Sigma$ and $\Delta^* \leftarrow \Sigma$ bands which are induced by a local translational mode of ca. 70 cm^{-1}. At elevated temperatures regular Σ and Δ bands have also been identified. This fact as well as the temperature dependence of the band shapes confirms that the radicals undergo (nearly) free rotation in the rare gas cage. Term values and intensity distributions are well reproduced by the calculations, if allowance is made for intensity borrowing by assigned and some unassigned Fermi resonances.

1. INTRODUCTION

The NH_2 radical exhibits a complex absorption spectrum in the visible and near-infrared region. The spectrum is due to an $\tilde{A}\,^2A_1 \leftarrow \tilde{X}\,^2B_1$ transition between states which become degenerate in the linear configuration. While the ground state is strongly bent, the excited state has a low barrier to linearity. The first thorough analysis of the spectrum was carried out by Dressler and Ramsay (*1*). The results of this and related studies were summarized by Herzberg (*2*). Three investigations of the visible spectrum of matrix-isolated NH_2 have also been reported (*3–5*). Information on high vibronic levels of the ground state, which cannot be obtained by classical absorption spectroscopy, became accessible by laser-induced fluorescence techniques (*6*), which also yielded detailed information on radiative lifetimes and quenching rate constants in the $\tilde{A}\,^2A_1$ state (*7, 8*). Very detailed information on high levels of the bending vibration v_2 and its combinations with the symmetric and asymmetric stretching vibrations v_1 and v_3 in the electronic groundstate was recently obtained by a combination of laser-induced fluorescence excitation with high-resolution FT spectrometry (*9*). Difficulties in the interpretation of the visible spectrum of such a simple radical arise from the fact that near resonant rovibronic levels of the same symmetry, but belonging to different electronic states, are mixed by Renner–Teller interaction. Further perturbations arise from Fermi resonances in the electronically excited state between levels of the bending vibration and its nearly degenerate combinations with the symmetric stretch (*1*), but also in the ground state (*9, 10*).

A considerable amount of theoretical work has been devoted to the NH_2 radical. Of great importance for the interpretation of the visible absorption spectrum has been

[1] Permanent address: Institute of Physical Chemistry, Faculty of Sciences, Studentski trg 12, 11000 Beograd, Yugoslavia.

0022-2852/93 $5.00

the approach of Jungen *et al.* (*11–13*), who constructed Born–Oppenheimer potential curves from available spectroscopic data. These were used to calculate term values, vibronic spin–orbit coupling constants, and relative transition probabilities which, when combined with ab initio calculations, can be utilized to obtain radiative lifetimes or absorption cross sections. It has been shown that the potential curves of Jungen *et al.* are in close agreement with those generated by modern ab initio techniques (*14*).

While experimental information on term values is rapidly increasing, comparison data for theoretical transition probabilities are rather scarce (*12, 15*). As shown in Section 4 of this paper, the $\tilde{A}\,^2A_1 \leftarrow \tilde{X}\,^2B_1$ spectrum of gaseous NH_2 simplifies considerably when the radical is isolated at low temperatures in a rare gas matrix. Thus, integrated band intensities can be determined much more rapidly in low-temperature matrices than in the gas phase, where band intensities are smeared out over a large number of congested lines. Vibronic term values obtained by theoretical methods are very helpful in assigning matrix spectra with narrow linewidths and small matrix shifts, i.e., commensurate with the uncertainty range of the theoretical approach. These conditions are ideally met by matrix-isolated NH_2 (*4*). Furthermore, the theoretical methods mentioned above can be adapted to calculate spectroscopic constants for the deuterides NHD and ND_2, which have been scarcely studied in the gas phase (*1, 16*). This motivated us to measure absorption spectra of matrix-isolated NH_2, NHD, and ND_2, and to compare the results with computations of vibronic term values, vibronic spin–orbit coupling constants, and vibronic transition moments.

The paper is organized as follows: Experimental procedures are described in Section 2. Section 3 briefly reviews the theoretical procedures employed for calculating term values, vibronic spin–orbit coupling constants, and vibronic transition moments of the $\tilde{A}\,^2A_1 \leftarrow \tilde{X}\,^2B_1$ systems of NH_2, ND_2, and NHD. These data, in conjunction with complementary information from gas-phase and matrix studies, are utilized in Section 4 to assign and interpret the obtained absorption spectra, and to assess the validity of the computational procedures described in Section 3. The paper ends with a summary.

2. EXPERIMENTAL DETAILS

Experiments were performed in a He transfer cryostat. Typically 80 mmole of a rare gas were premixed with 0.02–0.2 mole% NH_3 (Linde, 99.95%), or ND_3 (MSD, stated isotopic purity 99.4%), and sprayed on a polished platinum surface at 15 K. The matrices were photolyzed 10–12 hr at 14–15 K through the sapphire window of a microwave-powered Ar/Br_2 lamp, which emits several intense lines in the 149–164 nm range. Annealing times and temperatures (e.g., $\leq$15 min at 30 K in argon) represented a compromise between the reduction of heterogeneous line broadening on the one hand, and radical losses by diffusion/reaction on the other.

Simultaneous absorbance measurements of the NH $A^3\Pi \leftarrow X^3\Sigma^-$ (0, 0) band at 338 nm (transition moment $B_{12} = 3.7 \times 10^{18}$ m^3 J^{-1} sec^{-2}, based on lifetime measurements (*18*)) and of prominent NH_2 $A^2A_1 \leftarrow X^2B_1$ bands (transition moments from (*19, 20*)) as function of photolysis time revealed that, under the conditions of this study, photolysis of matrix-isolated NH_3 yielded approximately equal amounts of NH_2 and NH. After several hours of photolysis the NH_2:NH ratio decreased, probably due to secondary photolysis of NH_2, while the absolute NH_2 column density still increased. NH_2 column densities of $\approx 10^{18}$ cm^{-2} in Ar have been achieved, which corresponds to a conversion efficiency $NH_3 \rightarrow NH_2$ in the order of 17%.

Absorption spectra were recorded by illuminating the matrix with a stabilized 10 W tungsten halogen lamp. The light reflected from the polished platinum support of the matrix was focused on the entrance slit of a Spex 1402 double monochromator (gratings 1200 grooves/mm, blazed for 500 nm, chosen nominal resolution ca. 0.1 nm). The dispersed radiation was detected with a cooled photomultiplier (Hamamatsu R943-02) using an electrometer, or alternatively photon counting electronics. Spectra were calibrated by superimposing emission lines of various Pen-Ray lamps. All line positions reported in this paper are given as wavenumbers *in vacuo* (cm^{-1}).

In order to convert an obtained spectrum $I_{(\lambda)}$ into the desired naperian absorbance spectrum $B_{(\lambda)} = \ln(I_0/I)_\lambda$, it had to be divided by the corresponding unattenuated lamp spectrum $I_{0(\lambda)}$. The latter was provided by fitting a smooth contour to the experimental spectrum $I_{(\lambda)}$, which consisted of relatively widely spaced narrow absorption features superimposed on the structureless $I_{0(\lambda)}$ spectrum of the tungsten halogen lamp. However, because absorption spectra were recorded in the reflection mode to increase the optical path, a scattering correction had to be introduced for the opacity of the matrices. From residual intensities underneath strong absorption features it was estimated that only 80–93% of the unattenuated radiation between the NH_2 absorption lines had been reflected by the platinum surface, while 20 to 7% of the signal was due to scattering at or very near the matrix surface. The dynamic range of the measurements was increased by preparing matrices with low and high NH_2 column densities.

3. THEORETICAL CALCULATIONS

In our calculations of vibronic term values, intensity distributions, and spin–orbit splittings in NH_2, NHD, and ND_2 spectra we employ the potentials for the bending vibrations in the $\tilde{X}\,^2B_1$ and $\tilde{A}\,^2A_1$ electronic states, together with other relevant structure parameters, which were derived by Jungen *et al.* from spectroscopic data of the light isotopomer NH_2 (*12*). The theoretical approach has been described in detail elsewhere (*14, 21*), and only a brief summary is given here: We adopted the Hamiltonian derived by Bunker and co-workers (*22, 23*), which applies to large-amplitude bending vibrations of triatomic molecules, and incorporates the leading part of the bend–stretch interaction. The Hamiltonian is thus appropriate for treating the problem of the $\tilde{X}\,^2B_1$ and $\tilde{A}\,^2A_1$ electronic states of NH_2, which are coupled via the Renner–Teller effect. It is assumed that the stretching vibrations as well as the rotations around the axes perpendicular to a, which denotes the axis of smallest moment of inertia, can be separated. Thus, the problem of Fermi resonances is excluded from our treatment. The projection of total angular momentum (excluding spin) on the a-axis, which coincides with the molecular axis in the linear configuration, is assumed to be conserved, i.e., K is treated as a good quantum number.[2]

The remaining degrees of freedom (electronic motion, bending, and a-axis rotation) are treated simultaneously. Our vibronic treatment is the same as that of Jungen *et al.* (*11–13*). However, instead of numerically, we solve the Schrödinger equation variationally, employing as basis the eigenfunctions of a two-dimensional harmonic oscillator, multiplied by the electronic wavefunctions of the two states in question, and by the functions describing rotation around the a-axis. In a previous study (*14*) it has been shown that the largest discrepancies between the results obtained by em-

[2] In the calculations we identify K with the asymmetric-top quantum number K_a. The validity of this approximation has been discussed, e.g., by Carter and Handy (*24*).

ploying these two approaches do not exceed 1–2 cm^{-1} in the energy range up to 30 000 cm^{-1}.

While the computed term values for NH_2 agree with observations in the gas phase within 20 cm^{-1}, the agreement for ND_2 and NHD, which were not considered in the work of Jungen *et al.*, is significantly poorer. This is not surprising, since the bending potentials derived by fitting the Bunker–Landsberg semirigid-bender Hamiltonian (*23*) to term values of NH_2 are not strictly isotopically invariant, e.g., because the equilibrium bond lengths involved in the kinetic energy expression represent averages over the stretching vibrational states. However, the relatively large discrepancies for the heavier isotopomers could as well be an indication for the cancellation of errors in the operators for the kinetic and potential energies within the model employed by Jungen *et al.* (*12*) by fitting experimental data for NH_2 only, and/or may arise because the effective one-dimensional treatment of the bending motion in the framework of the semirigid-bender formalism cannot account satisfactorily for the existing bend–stretch coupling; see the results in Section 4.

An alternative way to compute the vibronic term values of the $\tilde{X}\,^2B_1$ and $\tilde{A}\,^2A_1$ states consists in using ab initio calculated potentials. The advantage of this approach is that one is not forced (at least in principle) to assume *any* model (as, e.g., the one-dimensional vibrational treatment), and that the estimation of some quantities (e.g., electronic transition moments) and parameters required in particular models (such as the variation of the equilibrium bond length with the bond angle, which is involved in the Bunker–Landsberg Hamiltonian) is straightforward and in general more reliable than their derivation from experimental data (*19*). A serious drawback of pure ab initio calculations, however, is their limited accuracy (typical errors in the computation of energy differences between electronic states amount to 0.1 eV). For this reason we employ the empirical potentials of Jungen *et al.* (*12*) in the present study, rather than ab initio data. An extensive analysis of this problem, in connection with the computation of vibronically averaged hyperfine coupling constants in NH_2, can be found in a recent paper by Perić and Engels (*25*).

In their computation of the intensity distribution in the $\tilde{A}\,^2A_1 \leftrightarrow \tilde{X}\,^2B_1$ system of NH_2 Jungen *et al.* (*12*) employed an electronic transition moment function of the simple form $\mu_e(\rho) = \mu_e^{(0)} \cdot \sin(\rho/2)$ ($\rho = \Pi$ − bond angle), which was found to be in reasonable agreement with ab initio calculations (*12, 19*). They neglected the diagonal transition moments (i.e., dipole moments) $\langle \tilde{X}\,^2B_1 \| \tilde{X}\,^2B_1 \rangle$ and $\langle \tilde{A}\,^2A_1 \| \tilde{A}\,^2A_1 \rangle$, which also contribute to the vibronic transition probability via the Renner–Teller coupling. The computations of the intensity distributions in the visible absorption spectrum, *vide infra*, confirm the validity of this approximation. This is because the lowest $K = 0$ and $K = 1$ vibronic levels of the ground electronic state $\tilde{X}\,^2B_1$ (from which absorption starts in the present experiments), lying 7000 to 8000 cm^{-1} below the barrier to linearity, are entirely ($K = 0$) or practically ($K = 1$) decoupled from the levels belonging to the upper electronic state, and since the probability for transitions between them and vibronic levels belonging in zeroth-order approximation (i.e., without Renner–Teller coupling) to the same (i.e., the $^2B_1$) electronic state is very small because of the unfavorable Franck–Condon factors; e.g., the probability for a transition from the $v_2'' = 0$ ($K = 0$) level to a $K = 1$ level belonging predominantly to the $^2B_1$ electronic species is practically determined by the amount of admixture of the $^2A_1$ electronic state to the vibronic wavefunction of the upper level.

We have already mentioned the fact that the empirical potentials of Jungen *et al.* (*12*) are not exactly isotopically invariant, with the consequence that the discrepancies between computed vibronic term values for ND_2 and NHD and their experimentally derived counterparts are in some cases as large as 100 cm^{-1}. These relatively large discrepancies prevent a reliable description of properties such as vibronic transition probabilities and spin–orbit splittings, which depend strongly on the composition of the vibronic wavefunction in cases where two $K \neq 0$ vibronic levels, belonging predominantly to different potential surfaces ($^2B_1$ and $^2A_1$), lie close to each other. This should be kept in mind when comparing the results of our theoretical calculations with experimental data.[3]

4. EXPERIMENTAL RESULTS AND DISCUSSION

NH_2 in Different Rare Gases

Absorption spectra of matrix-isolated NH_2 consist of narrow lines of typically 3–5 cm^{-1} width. Some linewidths could be reduced below 2 cm^{-1} by careful annealing. Figure 1 compares a small portion of the spectra in Ne, Ar, Kr, and Xe matrices with

[3] See Tables II, IX–XI, and Fig. 7 appearing later.

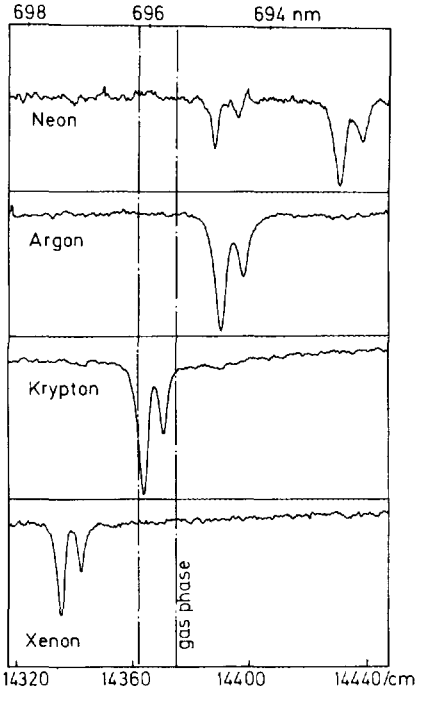

FIG. 1. Resolved inverted spin doublet of the 2+ II transition of NH_2 in different rare gas matrices at 5 K. The F_1, F_2 components of the $^RR_{00}$ line in the gas phase are indicated by dashed lines.

the position of the corresponding ${}^{R}R_{00}$ spin doublet of the 2+ Π band in the gas phase[4] (*1*). Note that the vibronic matrix shifts for this line are rather small and follow a regular trend from -30 cm^{-1} in the heaviest most polarizable rare gas xenon to $+65$ cm^{-1} (site I) in the lightest least polarizable rare gas, neon. A second less abundant and less blue-shifted site II was discovered in Ne matrices, which does not exist in the other rare gases. These findings are in line with a recent study of matrix-isolated NH, which was also generated by *in situ* photolysis of NH_3 (*26*). The magnitude of the spin splitting is found to be the same in the four rare gas matrices within our error limits of about 0.5 cm^{-1}. Deviations from the splitting in the gas phase will be considered below. Table I summarizes the matrix shifts of those Π bands which have been observed in the gas phase and in all rare gases: the matrix shifts are always much less than 0.5%.

Assignment of NH_2 Spectra in Argon

Apart from small matrix shifts, no significant differences were observed between absorption spectra of NH_2 in different rare gas matrices. For this reason the following discussion focuses on the spectra in Ar matrices. Survey spectra in this rare gas at 5 and 22 K, covering the wavenumber range from 11 000 to above 27 000 cm^{-1}, are shown in Figs. 2 and 3. The 5-K spectrum is in excellent agreement with an earlier photographic recording of Robinson and McCarty at 4.2 K (*4*), in spite of the fact that these authors prepared NH_2 rather unselectively in a microwave-discharge of 4%

[4] Since the excited state of NH_2 is quasilinear, quantum numbers of the bending vibration v_2' may be expressed in "linear" or "bent" notations. The relation is $v'_{2(\text{lin.})} \triangleq 2v'_{2(\text{bent})} + K'_a + 1$. We use v_2 quantum numbers in the "bent" notation; "minus" and "plus" signs distinguish between levels belonging to the lower ($V^- \triangleq \tilde{X}\,{}^2B_1$) and upper ($V^+ \triangleq \tilde{A}\,{}^2A_1$) bending potentials. The rotational level notation is $N_{Ka\,Kc}$, where N denotes total angular momentum exclusive of spin. Rotational lines are designated ${}^{\Delta Ka}\Delta N_{Ka,Kc}$ (*1*).

TABLE I

Matrix Shifts ($\bar{\nu}_{\text{matrix}} - \bar{\nu}_{\text{gas}}$) $\equiv \Delta\bar{\nu}_{\text{mg}}$ of Prominent Π Bands of NH_2 in Ne, Ar, Kr, and Xe, in [cm^{-1}]. Gas-Phase Data from (*1, 17*)

NH_2, Π band	$\bar{\nu}_{\text{gas}}$, ${}^{R}R_{00}$	$\Delta\bar{\nu}_{\text{mg}}$, Ne I	$\Delta\bar{\nu}_{\text{mg}}$, Ne II	$\Delta\bar{\nu}_{\text{mg}}$, Ar	$\Delta\bar{\nu}_{\text{mg}}$, Kr	$\Delta\bar{\nu}_{\text{mg}}$, Xe
1+	12643	66	22	22	− 5	− 32
2+	14368	65	23	24	− 2	− 30
3+	15901	66	19	32	− 10	− 32
4+	17559	79	29	29	− 7	− 41
1,2+,0	17756	81	24	17	− 22	− 61
1,3+,0	19227	86	28	17	− 25	− 67
5+	19394	80	27	17	− 20	− 61
6+	21215	80	21	5	− 39	− 82

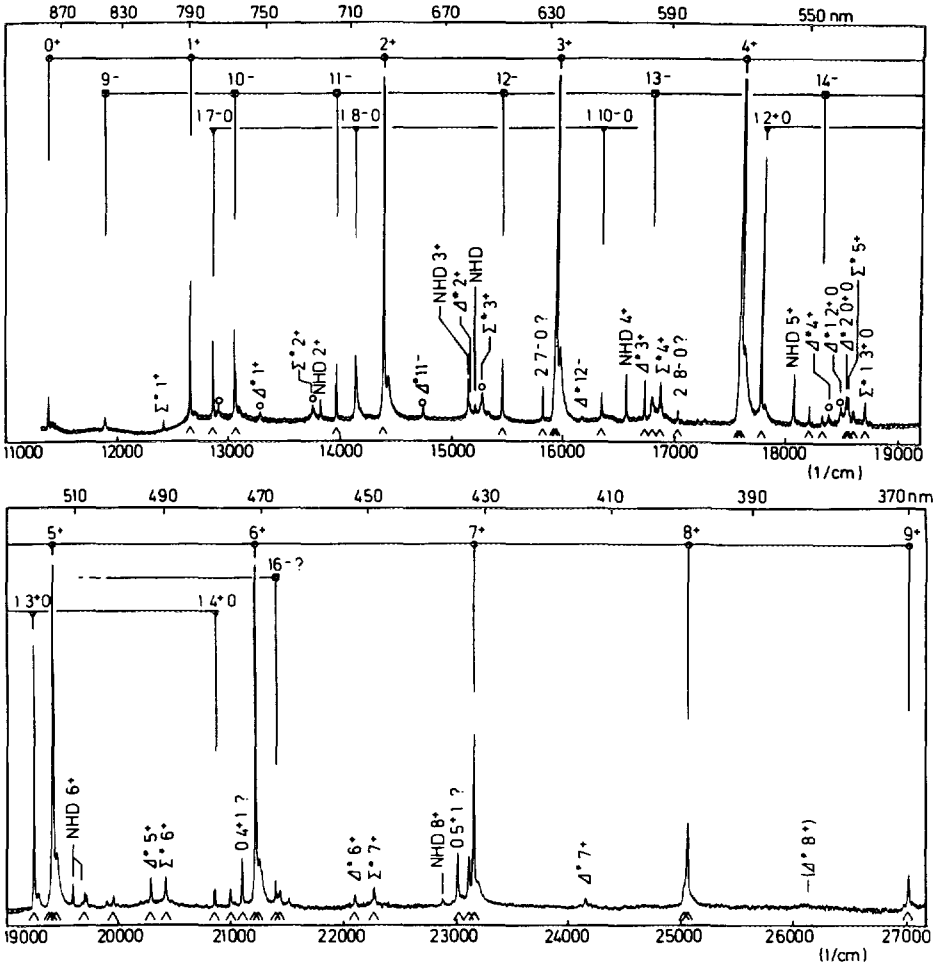

FIG. 2. Low temperature (5 K) absorption spectrum of matrix-isolated NH_2 in argon, showing Π progressions of the v_2 bending vibration and combination bands with the symmetric stretch v_1. NHD is present as an impurity from a previous experiment with ND_3. Bands marked with ∧ are also reported in Table I of Ref. (*4*), while those marked with 0 are not. Asterisks indicate matrix-induced $\Sigma^* \leftarrow \Sigma$ and $\Delta^* \leftarrow \Sigma$ transitions.

N_2H_4 in argon, while in our case photolysis of matrix-isolated NH_3 was employed at considerably lower mixing ratios as a clean source of matrix-isolated NH_2. The other photolysis products (H, H_2, NH) are either removed by annealing, or are practically nonabsorbing in the spectral range of interest (*27*). Nearly all the lines reported by Robinson and McCarty, including those which could not be assigned at their time, are recovered in our spectrum, confirming their association with NH_2. Note that some weak lines, which we also attribute to NH_2 in our low temperature spectrum, are not reported in Table I of Robinson and McCarty. These authors listed only those lines which, "because of their sharpness, intensity, and insensitivity to the oxygen impurity could be reasonably attributed to NH_2" (*4*).

Our assignment of the low-temperature NH_2 spectrum in argon confirms and extends previous matrix work (*3–5*). Robinson and McCarty have shown that the strongest

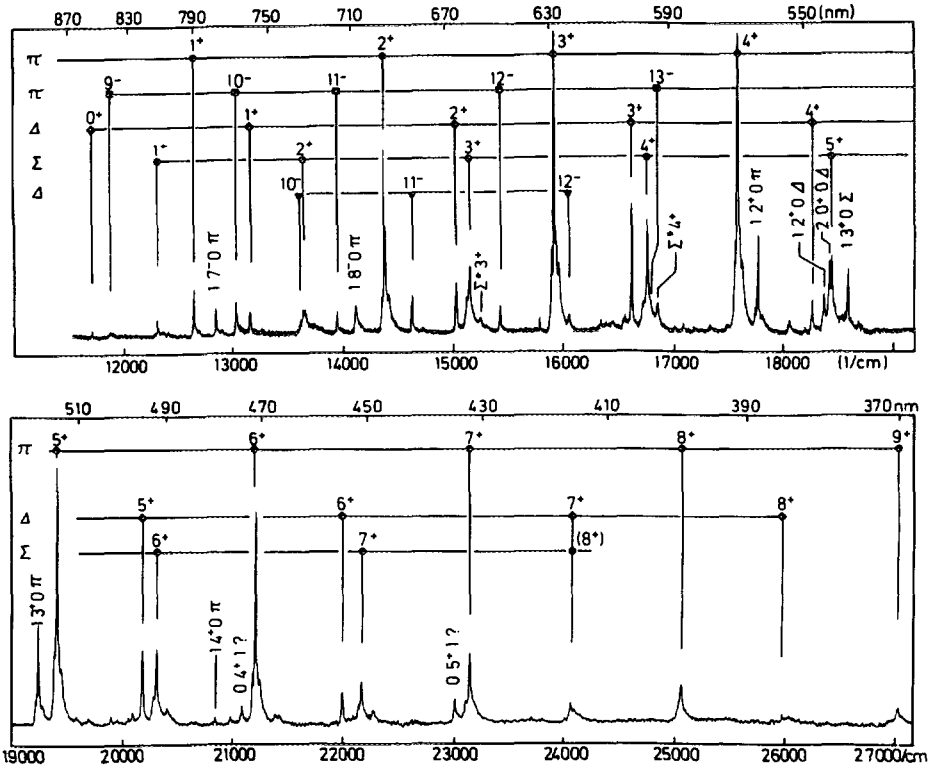

FIG. 3. High-temperature (22 K) absorption spectrum of matrix-isolated NH_2 in argon, showing Π, Σ, and Δ progressions of the bending vibration v_2 and its combinations with the symmetric stretch v_1.

lines are in very good agreement with Dressler and Ramsay's analysis of the NH_2 absorption spectrum in the gas phase (*1*) if the following assumptions are made:

(a) Matrix-isolated NH_2 is a free rotor in the matrix cage, which obeys the rotational selection rules;

(b) the o ↔ p conversion by flipping a hydrogen's nuclear spin, which is forbidden by the $s \leftarrow/\rightarrow a$ selection rule, is fast in the matrix on the experimental time scale.

We present evidence that assumption (a) is a good working hypothesis, but is not strictly valid due to weak rotation–translation coupling in the rare gas cage. Assumption (b) implies that the lowest *symmetric* rotational level 1_{01} of the $\tilde{X}\,^2B_1$ state (gas-phase term value 21.1 cm^{-1}) is totally relaxed to the lowest *antisymmetric* rotational level 0_{00}, which thus becomes the only absorbing level at 5 K. Assumption (a) implies that the $\Delta K_a = \pm 1$ selection rule is valid, and that only Π bands can be observed at this temperature, i.e., vibronic transitions to levels with $K'_a = +1$ (cf. Fig. 7 in Ref. (*1*)), each transition consisting of a single $^RR_{00}$ line (or actually of a spin doublet). Because the radical is bent in the electronic ground state and quasi-linear in the excited state, the spectrum is dominated by a long progression of the bending vibration v'_2. Wavenumbers of the bands which are marked out in Fig. 2 are listed in Table II, together

TABLE II

NH_2 Π bands of the v_2' Bending Progression: Relative Vibronic Transition Moments Squared $|\langle v_2''|\sin(\rho/2)|v_2'\rangle|^2 = |TM|^2$, Theoretical $\bar{\nu}_{th}$, $\bar{\nu}_g$ in the Gas Phase ($^RR_{00}$ Lines, Means of Spin Doublets), $\bar{\nu}_m$ in Argon, and Corresponding Matrix Shifts $\Delta\bar{\nu}$. All Energies in [cm^{-1}]. Fermi-Perturbed Levels Marked "F" in Last Column

NH_2, Π band	$\|TM\|^2$ x 10^4	$\bar{\nu}_{th}$	$\bar{\nu}_g$	$\bar{\nu}_m$	$\Delta\bar{\nu}_{mg}$	$\Delta\bar{\nu}_{mth}$
0+	12	11322	11328[a]	11375	+ 47	+ 53
1+	48	12651	12643[a]	12665	+ 22	+ 14
2+	187	14345	14368[b]	14392	+ 24	+ 47
3+	383	15896	15901[a]	15933	+ 32	+ 37
4+	452	17587	17559[c]	17588	+ 29	+ 1 F
5+	363	19351	19394[c]	19411	+ 17	+ 60 F
6+	199	21186	21215[c]	21220	+ 5	+ 34 F
7+	82	23125	-	23143	-	+ 18
8+	30	25056	25050[d]	25052	- 2	- 4
9+	8	27035	27025[d]	27012	- 13	- 23
10+	0	29043	-	29012[e]	-	- 32

[a] (*17*); [b] (*28*); [c] (*1*); [d] (*12*); [e] Weak band reported in Ref. (*4*).

with calculated transition moments squared and term values, as well as $^RR_{00}$ line positions from recent gas-phase work (*1, 13, 17, 28*). The v_2' progression was observed all the way from $v_2' = 0+$ up to $v_2' = 9+$ (up to 10+ if a weak hitherto unassigned line in the spectrum of Robinson and McCarty is included (*4*)).

In addition to the well-known Fermi resonances between the 4+ and the 1, 2+, 0 bands, and between the 5+ and the 1, 3+, 0 bands (v_1 = symmetric stretch), another weaker Fermi resonance between 6+ and 1, 4+, 0 could be assigned. Both the estimated energy of the transition and the predicted intensity ratio, based on the known Fermi interaction constant (*1, 4, 29*) of the other resonances, support this assignment. Two sharp features at 21 100 and 21 005 cm^{-1}, which do not match with reasonable combinations of the bending and symmetric stretching vibrations, are in the approximate energy range of the 0, 4+, 1 and 0, 5+, 1 levels, if a recent estimate of the antisymmetric stretch of 3516 cm^{-1} in the $\tilde{A}\,^2A_1$ state is correct (*10*). These transitions are forbidden by the $\Delta v_3 = 0, \pm2, \pm4, \ldots$ selection rule in the gas phase (*30*), but may be induced by simultaneous excitation of an asymmetric local matrix mode. This hypothesis obtains further support from our observation of matrix-induced $\Sigma^* \leftarrow \Sigma$ and $\Delta^* \leftarrow \Sigma$ transitions, *vide infra*. Assigned and tentatively assigned transitions to v_1, v_2 combination levels which are in Fermi resonance with v_2 levels are listed in Table III.

Most members of the Renner–Teller induced Π transitions to v_2'' levels and to v_1'', v_2'' combination levels of the $\tilde{X}\,^2B_1$ state *above the barrier to linearity* have already

TABLE III

Fermi Resonances of Gas-Phase and Matrix-Isolated NH_2 in Argon (Π Bands, ${}^RR_{00}$ Lines, Means of Spin Doublets), Involving 0, v_2, 0 and 1, $v_2 - x$, 0 Levels ($x = 3$ in Ground State; $x = 2$ in Excited State). All Energies in [cm^{-1}]

resonances	$\bar{\nu}_g$	$\bar{\nu}_m$	$\Delta\bar{\nu}_{mg}$
1, 7−, 0	12871[a]	12865	− 6
0, 10−, 0	13027[b]	13058	+ 31
0, 11−, 0		13962	-
1, 8−, 0	(13971)[c]	14139	-
0, 3+, 0	15901[d]	15933	+ 3
0, 12−, 0	15459[e]	15443	− 16
2, 7−, 0	(15881)[c]	15811 tentative	-
1, 10−, 0		16356	-
0, 4+, 0	17559[f]	17588	+ 29
1, 2+, 0	17755[a]	17773	+ 18
1, 3+, 0	19227[f]	19244	+ 17
0, 5+, 0	19349[f]	19411	+ 17
1, 4+, 0		20859	
0, 6+, 0	21215[f]	21220	+ 5

[a] (*10*); [b]After Ref. (*12*); [c]extrapolation based on formula and vibrational constants in Ref. (*9*) for 1, v_2'', 0 combination bands, valid for $0 \leq v_2'' \leq 6$; [d](*17*); [e](*28*); [f](*1*).

been assigned by Ross *et al.* (*10*) in their recent reevaluation of McCarty and Robinson's matrix spectrum of NH_2 (*4*). Our Tables III and IV support their conclusions, and add transitions to the 9− and the combined 1, 10−, 0 levels. A line at 15 881 cm^{-1} is tentatively assigned to the 2, 7−, 0 level, borrowing its intensity from the strong Π transition to the 3+ level of the $\tilde{A}\,{}^2A_1$ state, while another line at 15 236 cm^{-1} would be in the appropriate energy range of the 1, 9−, 0 transition. However, although the 1, 10−, 0 transition was observed, the assignment of the 1, 9−, 0 transition had to be discarded, because the line in question could be shown to arise from a matrix-induced $\Sigma^* \leftarrow \Sigma$ transition, *vide infra*. Ross *et al.* (*10*), who associate a line at 16 800 cm^{-1} in Table I of Ref. (*4*) with the 13− Π band, in accordance with our analysis, could not exclude an alternative assignment to a line at 16 873 cm^{-1}. We can show that this line arises from a matrix-induced $\Sigma^* \leftarrow \Sigma$ transition, and thus cannot represent the 13− Π line. Guided by the theoretical term values and transition moments squared in columns 2 and 3 of Table IV, two weak features at 18 328 and 21 398 cm^{-1} may be tentatively assigned to the $K_a = 1$ levels of 14− and 16−.

We have briefly investigated the effect of the matrix gas on Fermi resonances by determining interaction constants W_{ni} from intensity ratios (*29*). The following interaction constants (averages of two independent determinations) were obtained for the resonances between the 4+ and 1, 2+, 0 level pairs ($W_{ni} \equiv W4$), and between the 5+ and 1, 3+, 0 level pairs ($W_{ni} \equiv W5$):

TABLE IV

Renner-Teller Induced II Progressions of the Bending Vibration ν_2 in the $\tilde{X}\,^2B_1$ State of NH_2: Relative Vibronic Transition Moments Squared $|TM|^2$, Theoretical $\bar{\nu}_{th}$, $\bar{\nu}_g$ in the Gas Phase, $\bar{\nu}_m$ in Argon Matrix, and Corresponding Matrix Shifts $\Delta\bar{\nu}$. All Energies in [cm^{-1}]. "t" Indicates Tentative Assignment; Fermi-Perturbed Levels Marked "F" in Last Column

NH_2, II band	$\lvert TM\rvert^2$ x 10^4	$\bar{\nu}_{th}$	$\bar{\nu}_g$	$\bar{\nu}_m$	$\Delta\bar{\nu}_{mg}$	$\Delta\bar{\nu}_{mth}$	
9-	7	11847	11889[a]	11892	+ 3	+ 45	
10-	44	12990	13038[a,b]	13058	+ 20	+ 68	F
11-	57	14045		13962	-	- 83	F
12-	28	15449	15463[c]	15443	- 20	- 6	
13-	14	16883	16827[c]	16800	- 27	- 83	
14-	9	18357	-	18328 t	-	- 29	
15-	8	19867	-	-	-	-	
16-	17	21416	-	21398 t	-	- 18	
17-	11	22940	-	-	-	-	
18-	1	24537	-	-	-	-	

[a] (9); [b] (12); transition showing "strong anharmonic effects"
[c] (10).

*W*4:

Ne I, 68 ± 0.5 cm^{-1}; Ne II, 71.5 ± 1.5 cm^{-1}; Ar, 62.5 ± 1.5 cm^{-1};

Kr, 68.7 ± 1 cm^{-1}; Xe, 68.2 ± 0.5 cm^{-1};

*W*5:

Ne I, 71.9 ± 1 cm^{-1}; Ne II, 68.5 ± 1 cm^{-1}; Ar, 70.1 ± 2 cm^{-1};

Kr, 73.3 ± 2 cm^{-1}; Xe, 70.2 ± 1 cm^{-1}.

No significant trend can be derived from these data, which are in reasonable agreement with another estimate of $W4 = 71.8$ cm^{-1}; $W5 = 75.7$ cm^{-1} for NH_2 in argon (*4*), and close to the gas-phase estimate of $W = 72 \pm 3$ cm^{-1} (*1*).

When the matrix temperature is raised to 22 K, higher symmetric and antisymmetric rotational levels can be thermally populated in the electronic ground state. This "broadens" the II bands (which consisted of a single resolved or unresolved spin doublet at 5 K) by adding two rotational lines arising from the symmetric 1_{01} level, and gives rise to (likewise "broadened") Σ as well as narrower Δ bands (cf. Figs. 6–8 in Ref. (*1*)). These considerations, in conjunction with gas-phase data, calculated band positions, and relative vibronic transition moments, enabled us to assign most of the "high-temperature" features in the spectrum of matrix-isolated NH_2 in argon,

Fig. 3, to Σ and Δ progressions of the bending vibration and its combination bands with the symmetric stretch, v_1. The results are listed in Tables V and VI. Significant deviations from the smooth variation of $\Delta\bar{\nu}_{mth}$ ($\bar{\nu}_m$ = transition energy in the matrix; $\bar{\nu}_{th}$ = theoretical term value) occur for those levels which are known to be perturbed by Fermi resonances.

Matrix-Induced $\Sigma^* \leftarrow \Sigma$ *and* $\Delta^* \leftarrow \Sigma$ *Transitions*

While all of the stronger features in the NH_2 low-temperature spectrum in argon could be assigned (or tentatively assigned) to $\tilde{A}\,^2A_1$ or $\tilde{X}\,^2B_1$ state levels of the bending vibration and its combinations with the symmetric stretch, many weaker lines, which appear quite regularly between the Π bands of the intense v_2' progression, do not fit this level scheme at all if only $K_a = 1$ levels are considered in the upper states. Comparison of Figs. 2 and 3 shows clearly that the relative intensities and positions of these lines[5] which could not be assigned to Π transitions are superficially similar to, but not coincident with, the v_2' Σ and Δ bands of the high temperature spectrum. A

[5] These lines must not be confused with additional "hot" lines in the matrix spectrum of McCarty and Robinson (*4*), which were *not* observed in our low-temperature spectrum. We suspect that these "hot" absorptions were due to temperature inhomogeneities in the strongly irradiated matrix, as already suspected by these authors.

TABLE V

NH_2 Σ Bands of the v_2' Bending Progression: Relative Vibronic Transition Moments Squared $|TM|^2$, Theoretical $\bar{\nu}_{th}$, $\bar{\nu}_g$ in the Gas Phase ($^PQ_{11}$ Lines), $\bar{\nu}_m$ in Argon, and Corresponding Matrix Shifts $\Delta\bar{\nu}$. All Energies in [cm^{-1}]. Fermi-Perturbed Levels Marked "F" in Last Column

NH_2, Σ band	$\lvert TM\rvert^2$ x 10^4	$\bar{\nu}_{th}$	$\bar{\nu}_g$	$\bar{\nu}_m$	$\Delta\bar{\nu}_{mg}$	$\Delta\bar{\nu}_{mth}$
1+	51	12280	12267[a]	12326	+ 59	+ 46
2+	165	13617	13605[a]	13653	+ 48	+ 36
3+	383	15121	15106[a]	15165	+ 60	+ 44
4+	452	16754	16728[a]	16777	+ 49	+ 23 F
1,2+,0	-	-	17059[b]	17098	+ 39	
5+	363	18485	18416[a]	18454	+ 38	- 31 F
1,3+,0	-	-	18570[a]	18603	+ 33	
1,4+,0	-	-	20075[a]	20100	+ 25	
6+	199	20293	20298[a]	20325	+ 27	+ 32 F
7+	82	22165	22163[a]	22171	+ 8	+ 6
8+	30	24087	24074[a]	weak		
9+	8	26051		v. weak		

[a] (1); [b] (17).

TABLE VI

NH_2 Δ Bands of the υ_2' Bending Progression: Relative Vibronic Transition Moments Squared $|TM|^2$, Theoretical $\bar{\nu}_{th}$, $\bar{\nu}_g$ in the Gas Phase ($^RR_{11}$ Lines), $\bar{\nu}_m$ in Argon, and Corresponding Matrix Shifts $\Delta\bar{\nu}$. All Energies in [cm^{-1}]. "w" Indicates Weak Feature, Large Error Limits; Fermi-Perturbed Levels Marked "F" in Last Column

NH_2, Δ band	$\|TM\|^2$ x 10^4	$\bar{\nu}_{th}$	$\bar{\nu}_g$	$\bar{\nu}_m$	$\Delta\bar{\nu}_{mg}$	$\Delta\bar{\nu}_{mth}$
0+	21	11676	11659[a]	11701	+ 42	+ 25
1+	87	13137	13143[a]	13178	+ 35	+ 41
2+	197	15036	15018[b]	15046	+ 28	+ 10
3+	390	16639	16608[b]	16637	+ 29	- 2
4+	412	18371	18256[b]	18282	+ 26	- 89 F
1,2+,0			18366[b]	18385	+ 19	
2,0+,0			18417[c]	18434	+ 17	
1,3+,0				19895		
5+	281	20179	20180[b]	20193	+ 13	+ 14 F
6+	104	22009	22004[b]	21999	- 5	- 10
7+	51	24063	-	24062 w	-	(- 1)
8+	16	26011	-	25967 w	-	(- 44)
10-	49	13612	-	13630	-	+ 18
11-	121	14638	-	14640	-	+ 2
12-	71	16117	16073[c]	16073	± 0	- 44
16-	52	22253	-	22273 w	-	(+ 20)

[a] (17); [b] (1); [c] (10).

closer inspection reveals that, wherever unidentified lines appear in Fig. 2, and similar "high-temperature" Σ and Δ bands appear in Fig. 3, the unidentified lines are blueshifted 101 ± 4 cm^{-1} from their high temperature counterparts. This is exemplified in Fig. 4, which shows a crowded section of the low- and "high"-temperature spectra of NH_2 in argon between 18 000 and 19 000 cm^{-1}. Only those peaks in the "high"-temperature spectrum which have been identified as Σ and Δ bands also appear in the low-temperature spectrum as Σ* and Δ* lines, but are shifted 100 cm^{-1} to higher energy. Note that the blueshifted * peaks are still detectable in the upper trace among the "high"-temperature Σ and Δ transitions, as indicated by the dashed vertical lines. The full set of Σ* and Δ* lines are also marked in Fig. 2. Their high-temperature counterparts are to be found in Fig. 3.

We assign the blueshifted * lines in the low temperature spectrum to matrix-induced "forbidden" transitions from the antisymmetric 0_{00} level of the electronic ground state to the same Σ and Δ levels which, at higher temperature, are accessible from the

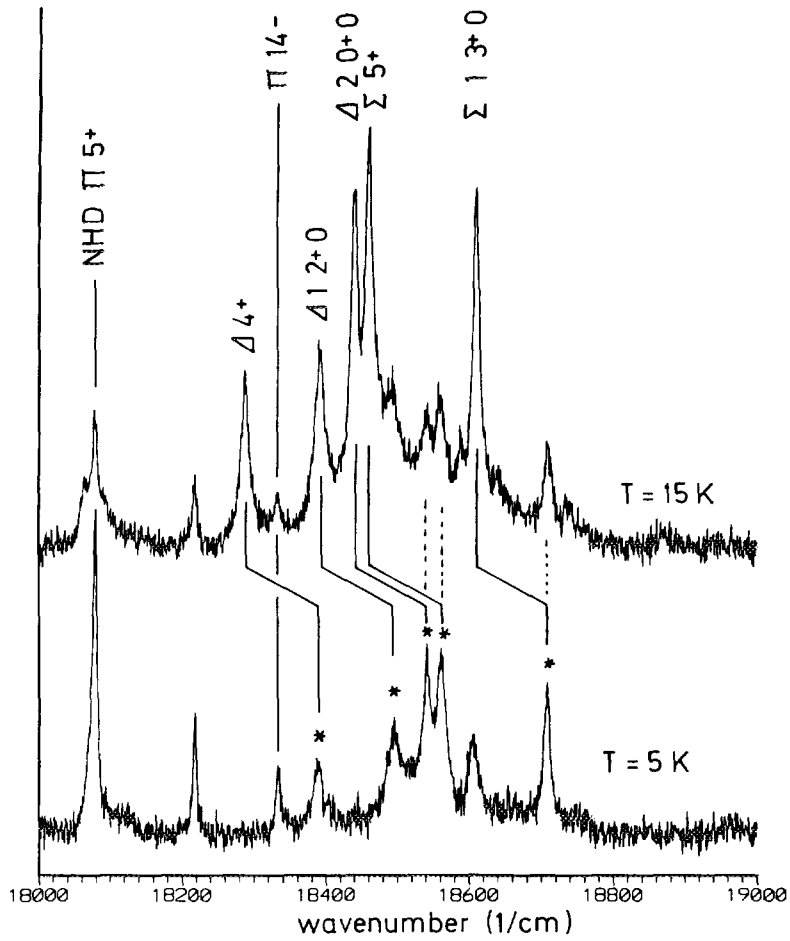

FIG. 4. Σ and Δ bands of NH_2 in argon at 15 K and the corresponding matrix-induced Σ* and Δ* bands at 5 K.

likewise antisymmetric 1_{11} level in an allowed transition. The blueshift arises from two contributions: (a) 32 cm^{-1} are gained from the separation between the two lowest antisymmetric rotational levels 0_{00} and 1_{11} in the absorbing ground state; (b) about 70 cm^{-1} are needed to excite a translational mode of NH_2 in its upper state. The frequency of 70 cm^{-1} agrees well with the translational mode of matrix-isolated NH, also a nearly free rotor in argon of nearly the same mass: the mode was identified as a prominent peak in the phonon sideband of the electric dipole forbidden matrix-induced $b\ ^1\Sigma^+$, $J' = 0 \rightarrow a\ ^1\Delta$, $\Omega = J'' = 2$ transition (*31*), and as a weak feature in the rotation–translation structure of the $a\ ^1\Delta \rightarrow X\ ^3\Sigma^-$ transition of this radical (*32*). The blueshifted Σ* and Δ* transitions of NH_2 become weakly allowed because the local mode contributes ± one unit of angular momentum.

We have tested this hypothesis by searching for similar Σ* and Δ* peaks in the low-temperature spectra of NHD and ND_2. For these radicals the 1_{11}–0_{00} separation in the ground state amounts to only 26 and 18 cm^{-1}, respectively, while the translational

mode frequencies should change very little. Unfortunately the spectra of the heavier isotopomers (a portion of the low-temperature spectrum is shown in Fig. 5), are much more crowded and overlapped by rather broad regular Σ and Δ bands of ND_2, even at 5 K, in the regions of interest. This made the search for Σ^* and Δ^* bands difficult. We have, however, positively identified the matrix-induced 6+ Σ^* and 5+ Δ^* bands of NHD which exhibit a blueshift of 95 ± 5 cm^{-1}, in excellent agreement with our hypothesis.

Assignment of NHD and ND_2 Spectra in Argon

Although the gas-handling system was carefully preconditioned with ND_3, the presence of NHD and even some NH_2 in the absorption spectra of ND_2 could never be fully eliminated. Figure 5 shows a representative portion of the low-temperature spectrum. The v_2' II progressions of the three isotopomers are marked out. A few transitions to $\tilde{X}\,^2B_1$ levels above the linearity barrier have also been identified. Due to the increasing density of states the number of accidental resonances between different II states is expected to increase in the order NH_2 < NHD < ND_2. While some of the v_1, v_2 combinations which borrow intensity from nearby II levels of the Franck–Condon allowed v_2' progression could be assigned, several other resonances remain unassigned. Furcate vertical bars in Fig. 5 denote groups of assigned and unassigned resonances which belong to the same isotopomer. The intensity ratios and spacings of the assigned resonances between the ND_2 level pairs 3+ ↔ (1, 1+, 0), 5+ ↔ (1, 3+, 0), and 6+ ↔ (1, 4+, 0) yielded reasonable Fermi interaction constants of $W3$ = 67 cm^{-1}, $W5$ = 61 cm^{-1}, and $W6$ = 60.5 cm^{-1}, respectively. Further resonances of the same series could not be definitely assigned because their intensity ratios and spacings would imply significantly smaller interaction constants, between W = 15 cm^{-1} and W = 30 cm^{-1}, and thus should belong to other series of interacting II levels.

Our assignments, including those of Σ and Δ bands at elevated temperatures, are listed in Tables VII–X. They are largely based on calculated vibronic term energies

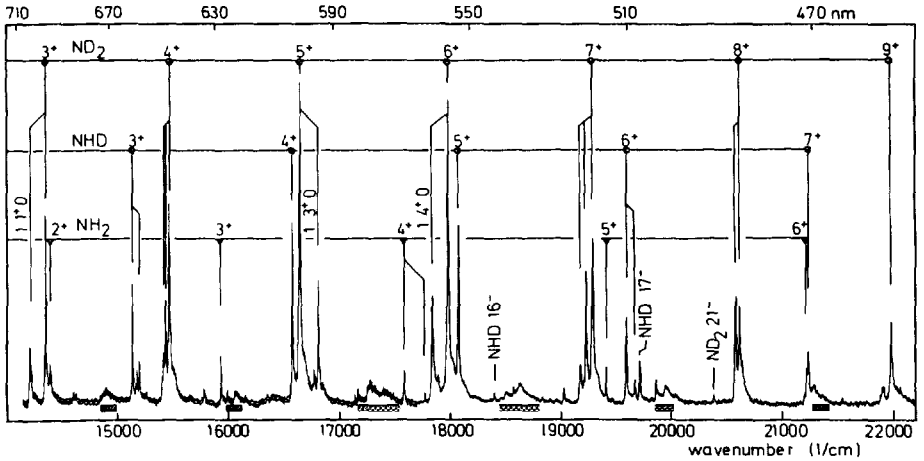

FIG. 5. Portion of a ND_2/NHD spectrum in argon at 5 K, showing essentially II progressions of the bending vibration v_2 (hatched horizontal bars indicate ranges of weak regular Σ and Δ bands). A few resonances with combined v_1, v_2 levels have been assigned. Other groups of unassigned resonances, which borrow intensity from nearby bands of the v_2' II progression, are also indicated.

TABLE VII

ND_2 II Bands of the ν_2' Bending Progression: Relative Vibronic Transition Moments Squared $|TM|^2$, Theoretical $\bar{\nu}_{th}$, $\bar{\nu}_g$ in the Gas Phase ($^RR_{00}$ Lines, Means of Spin Doublets (J)), $\bar{\nu}_m$ in Argon, and Corresponding Matrix Shifts $\Delta\bar{\nu}$. All Energies in [cm^{-1}]. Fermi-Perturbed Levels Marked "F" in Last Column

ND_2, II band	$\lvert TM\rvert^2$, x 10^4	$\bar{\nu}_{th}$	$\bar{\nu}_g$	$\bar{\nu}_m$	$\Delta\bar{\nu}_{mg}$	$\Delta\bar{\nu}_{mth}$
1+	11	12154	-	12154	-	0
13-	7	12441	-	12388?	-	- 53?
2+	30	13128	-	13131	-	+ 3
14-	36	13329	-	13269	-	- 60
1,1+,0				14209		
3+	138	14342	-	14352	-	+ 10 F
res.				15415		
res.				15436		
4+	281	15470	15400	15470	+ 70	± 0 F
5+	381	16676	16605	16642	+ 37	- 34 F
1,3+,0				16811		
1,4+,0				17849		
6+	381	17937	17949	17979	+ 30	- 42 F
res.				19175		
res.				19228		
7+	268	19237	-	19288	-	+ 51 F
21-	15	20455	-	20382?	-	- 73?
res.				20578		
8+	170	20611	-	20615	-	+ 4 F
9+	88	21983	-	21976	-	- 7
10+	35	23387	-	23360	-	- 27
11+	11	24814	-	24789	-	- 25
12+	3	26277	-	26231	-	- 46

and transition moments squared because comparison data from the gas phase are scarce, particularly for NHD. While our theoretical spectroscopic data for NH_2 are (and should be) practically identical with the results of Jungen *et al.* (*12*), theoretical data for ND_2 and NHD are presented for the first time in Tables VII–X. Note that only those theoretical data have been listed which can be compared with experimental results from this work. The complete set of theoretical results may be obtained upon request from one of the authors (M.P.).

TABLE VIII

ND_2 Σ Bands of the v_2' Bending Progression: Relative Vibronic Transition Moments Squared $|TM|^2$, Theoretical $\bar{\nu}_{th}$, $\bar{\nu}_g$ in the Gas Phase ($^PP_{10}$ Lines, Means of Spin Doublets (*1*)), $\bar{\nu}_m$ in Argon, and Corresponding Matrix Shifts $\Delta\bar{\nu}$. All Energies in [cm^{-1}]. Fermi-Perturbed Level Marked "F" in Last Column; "w" Indicates Weak Feature, Large Error Limits

ND_2, Σ band	$\|TM\|^2$, x 10^4	$\bar{\nu}_{th}$	$\bar{\nu}_g$	$\bar{\nu}_m$	$\Delta\bar{\nu}_{mg}$	$\Delta\bar{\nu}_{mth}$
2+	39	12809	-	12776	-	- 33
3+	113	13811	-	13782	-	- 29
4+	233	14910	14824	14897	+ 73	- 13
5+	353	16085	15995	16060	+ 65	- 25
6+	403	17321	17205	17256	+ 51	+ 65 F
1,4+,0			17341	17397	+ 56	
7+	354	18606	18569	18622	+ 53	+ 16
8+	242	19934	19905	19945	+ 40	+ 11
9+	132	21296	-	21282	-	- 14
10+	57	22689	-	22651 w	-	(- 38)
11+	20	24107	-	24047 w	-	(- 60)

Lineshapes and Spin Splitting

NH_2 is an often-cited example of a matrix-isolated free rotor, although the only reported matrix spectra (*3–5*) consist essentially of Π lines arising from the lowest 0_{00} level, with few weaker features being tentatively identified as Σ and Δ lines starting from the next higher rotational level(s) (*4*). How well the free rotor model actually applies to NH_2 and its isotopomers is depicted in Fig. 6, which shows lineshapes of the NH_2 6+, NHD 4+, and ND_2 5+ Π transitions in solid argon as a function of temperature. The gas-phase positions of the thermally induced $^RQ_{01}$ and $^RR_{01}$ lines, relative to the $^RR_{00}$ line in the matrix, are indicated. Note that the 1_{01} level of NHD is weakly, that of ND_2 appreciably populated even at 6 K. For ND_2 the *s* levels are additionally favoured by nuclear spin statistics, while the reverse holds true for NH_2.

Owing to the limited spectral resolution, and as a result of thermal line broadening at elevated temperature, the positions of Σ and Δ lines listed in the tables often refer to the maxima of broad features. It should be noted that the free rotor concept is valid only as an approximation because, even at the lowest temperature, weak phonon sidebands have been detected (cf. blue wings of the intense v_2' Π lines in Fig. 2, which do *not* coincide with "hot" $^RR_{01}$ lines). The induction of Σ* and Δ* bands by rotation–translation coupling is additional evidence that matrix-isolated NH_2 is not really a free rotor.

A previous investigation of the shapes of the $b\,^1\Sigma^+ \leftarrow X\,^3\Sigma^-$, $^QP_{(0)}$ lines of matrix-isolated NH and ND in Ar and Kr (*31, 33*), which were found to be essentially

TABLE IX

ND_2 Δ Bands of the ν_2' Bending Progression: Relative Vibronic Transition Moments Squared $|TM|^2$, Theoretical $\bar{\nu}_{th}$, $\bar{\nu}_g$ in the Gas Phase ($^RR_{10}$ Lines, Means of Spin Doublets (*1*)), $\bar{\nu}_m$ in Argon, and Corresponding Matrix Shifts $\Delta\bar{\nu}$. All Energies in [cm^{-1}]. Fermi-Perturbed Level Marked "F" in Last Column; "w" Indicates Weak Features, Large Error Limits

ND_2, Δ bands	$\lvert TM\rvert^2$, x 10^4	$\bar{\nu}_{th}$	$\bar{\nu}_g$	$\bar{\nu}_m$	$\Delta\bar{\nu}_{mg}$	$\Delta\bar{\nu}_{mth}$
1+	19	12455	-	12442	-	- 13
2+	54	13505	-	13550	-	+ 45
15-	64	14566	-	14604	-	+ 38
3+	152	14850	-	14847	-	- 3
16-	43	15612	-	15622	-	+ 10
4+	302	16009	15926	15990	+ 64	- 19
5+	374	17243	17130	17166	+ 36	+ 77 F
1,3+,0				17326		
6+	322	18526	18457	18498	+ 23	- 28
7+	146	19812	19847	19863	+ 16	+ 51
8+	121	21277	-	21201	-	- 76
9+	57	22659	-	22651 w	-	(- 8)
10+	20	24072	-	24047 w	-	(- 25)

homogeneous, implied that the lineshapes of matrix-isolated NH_2 were at least partially homogeneous at our spectral resolution. The widths must be due to fast matrix-induced relaxation processes. A preliminary search for laser-induced fluorescence of matrix-isolated NH_2 in argon, which was excited in the regions of the 1, 3+, 0, the 5+, and the 6+ II transitions with an excimer laser-pumped tunable dye laser, yielded extremely weak emission with a lifetime appreciably shorter than the pulse duration of the laser (≈20 nsec). The weak emission to rovibrational levels of the electronic ground state seemed to obey the $\Delta N = 0, \pm 2$ Raman selection rule, but further work is needed to confirm this preliminary conclusion. It is thus possible that we have observed resonance Raman emission.

Spin splitting could be resolved in a number of II and Δ bands of NH_2, and in a few II bands of ND_2 and NHD. The results and comparison data from the gas phase are listed in Table XI, together with theoretically calculated vibronic spin–orbit coupling constants $A_{v,K}$. These are based on ab initio computed $A^{SO} = f_{(\rho)}$, rather than on the empirically derived A^{SO} employed by Jungen *et al.* (*13*). At the linear geometry the ab initio value for A^{SO} ($-59.6\ cm^{-1}$) is higher than the corresponding value of Jungen *et al.* ($-50\ cm^{-1}$), which explains that our A_{vK} in Table XI are in general somewhat larger than the A_{vK} in Table 1 of Ref. (*13*). Spin splittings $\Delta F \equiv F_1 - F_2$ were calculated using Eq. (1) and $\bar{B}_{(v,K)}$ from Tables 1A or 5 in Ref. (*13*), and neglecting the *q*-

TABLE X

NHD II, Σ, and Δ Bands of the ν_2' Bending Progression: Relative Vibronic Transition Moments Squared $|TM|^2$, Theoretical $\bar{\nu}_{th}$, $\bar{\nu}_g$ in the Gas Phase (*16*), $\bar{\nu}_m$ in Argon, and Corresponding Matrix Shifts $\Delta\bar{\nu}$. All Energies in [cm^{-1}]. "w" Indicates Weak Features, Large Error Limits; Fermi-Perturbed Levels Marked "F" in Last Column

NHD II	$\lvert TM\rvert^2$, x 10^4	$\bar{\nu}_{th}$	$\bar{\nu}_g$, $^2R_{00}$	$\bar{\nu}_m$	$\Delta\bar{\nu}_{mg}$	$\Delta\bar{\nu}_{mth}$
1+	19	12336	-	12388 w	-	(+ 52)
11-	30	12642	-	12649	-	+ 7
12-	22	13478	-	13498	-	+ 20
2+	129	13813	-	13825	-	+ 12
3+	288	15137	-	15140	-	+ 3 F
res.				15200		
4+	409	16566	16546	16575	+ 29	+ 9
5+	405	18073	-	18074	-	+ 1
16-	16	18418	-	18400	-	- 18
6+	236	19624	-	19590	-	- 34 F
res.				19669		
17-	75	19755	-	19715	-	- 40
7+	165	21292	-	21235	-	- 57
8+	74	22951	-	22875	-	- 76
9+	25	24649	-	24502	-	-147
NHD Σ			$^0Q_{01}$			
3+	229	14492	-	14503	-	+ 11
4+	375	15872	15855	15905	+ 50	+ 33
5+	437	17341	17300	17345	+ 45	+ 4
6+	374	18881	-	18863	-	- 18
7+	240	20478	-	20427	-	- 51
NHD Δ			$^2R_{11}$			
3+	316	15752	15730	15759	+ 29	+ 7
4+	401	17228	17194	17211	+ 17	- 17
5+	331	18765	-	18732	-	- 33

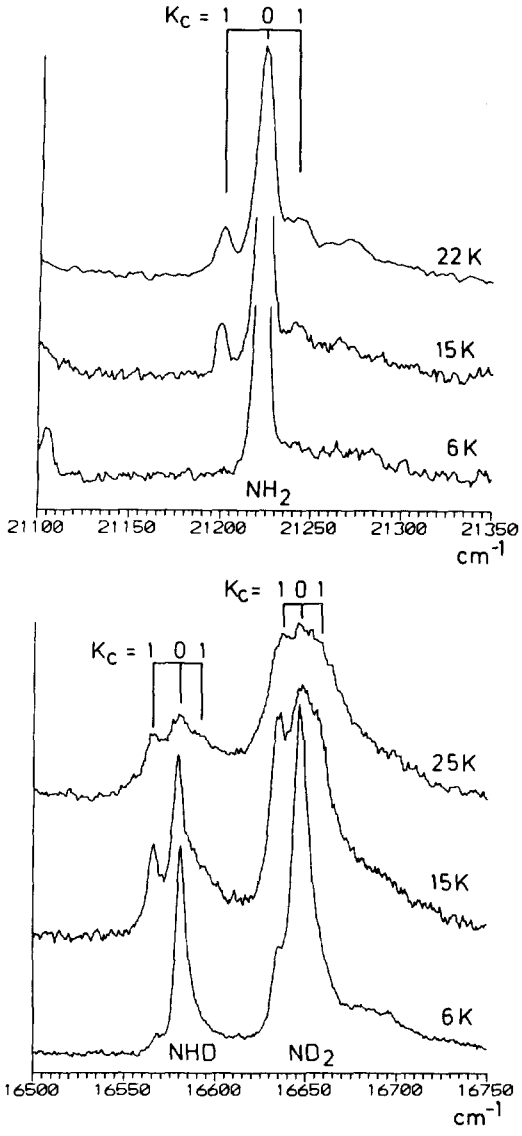

FIG. 6. Π bands of NH_2 (6+), NHD (4+), and ND_2 (5+), showing effect of temperature on relative populations of absorbing 0_{00} and 1_{01} levels. Gas-phase line positions are marked *relative* to the ${}^{R}R_{00}$ line in the matrix.

dependence. For the v_2+ levels of the deuterides we assumed $\bar{B}(ND_2) = 4.7\ cm^{-1}$ and $\bar{B}(NHD) = 6.4\ cm^{-1}$; the corresponding values for the v_2- levels are $\bar{B}(ND_2) = 5.45\ cm^{-1}$ and $\bar{B}(NHD) = 7.40\ cm^{-1}$. These estimates are related with $\bar{B}_{vK}(NH_2)$ via the ratios of the computed rotational constants in the linear configuration, $\bar{B}(NH_2) = 8.36\ cm^{-1}$, $\bar{B}(ND_2) = 4.19\ cm^{-1}$, and $\bar{B}(NHD) = 5.69\ cm^{-1}$.

Table XI shows that the splittings in the matrix, $\Delta F_{(matrix)}$, are on average somewhat smaller than $\Delta F_{(gas)}$. Where no gas-phase data are available for comparison, the agreement between $\Delta F_{(matrix)}$ and the calculations is in most cases still sufficient to support

TABLE XI

Calculated vs Observed Splittings $F_1 - F_2 = \Delta F$, of 1_1 and 2_2 Levels. Observations Pertain to II and Δ Bands in the Gas Phase (*10, 17*), and in Spectra of Matrix-Isolated NH_2, ND_2, and NHD in Solid Argon

NH_2	$\Delta F_{obs.}$ gas phase	$\Delta F_{obs.}$ matrix	A_{vg} calculated	$\Delta F_{calc.}$
0+ π	+ 2.0	+ 6.5	+ 9.96	+ 6.9
9- π	-	-14	-21.96	-18.2
1+ π	+ 9.5	+ 7.5	+14.66	+ 9.8
1,7-,0 π	-	- 3.5	-	-
10- π	-	- 9.5	-19.32	-15.7
11- π	-	+ 6	+12.29	+ 8.6
2+ π	-12.6	- 7.5	-14.00	-11.3
3+ π	- 4.8	- 3.5	- 5.80	- 4.5
0+ Δ	+ 8.4	+ 6	+ 9.98	+ 8.0
1+ Δ	+ 7.3	+ 8	+14.11	+11.2
11- Δ	-	+ 7	+13.06	+10.4
2+ Δ	-10.5	- 8.5	-14.59	-12.6
ND_2				
1+ π	-	+ 5.5	+11.86	+ 4.7
2+ π	-	+10.5	+14.01	+ 3.4
14- π	-	-17	-16.67	-14.1
3+ π	-	- 8	-10.82	- 9.0
4+ π	-	- 4.5	- 4.26	- 3.4
1,3+,0 π	-	- 4	-	-
NHD				
2+ π	-	- 5	-10.38	- 8.4
3+ π	-	- 2.5	- 3.69	- 2.9
16- π	-	- 4	- 4.17	- 3.2
6+ π	-	+ 6	+10.95	+ 7.1
17- π	-	- 6	-11.26	- 9.1

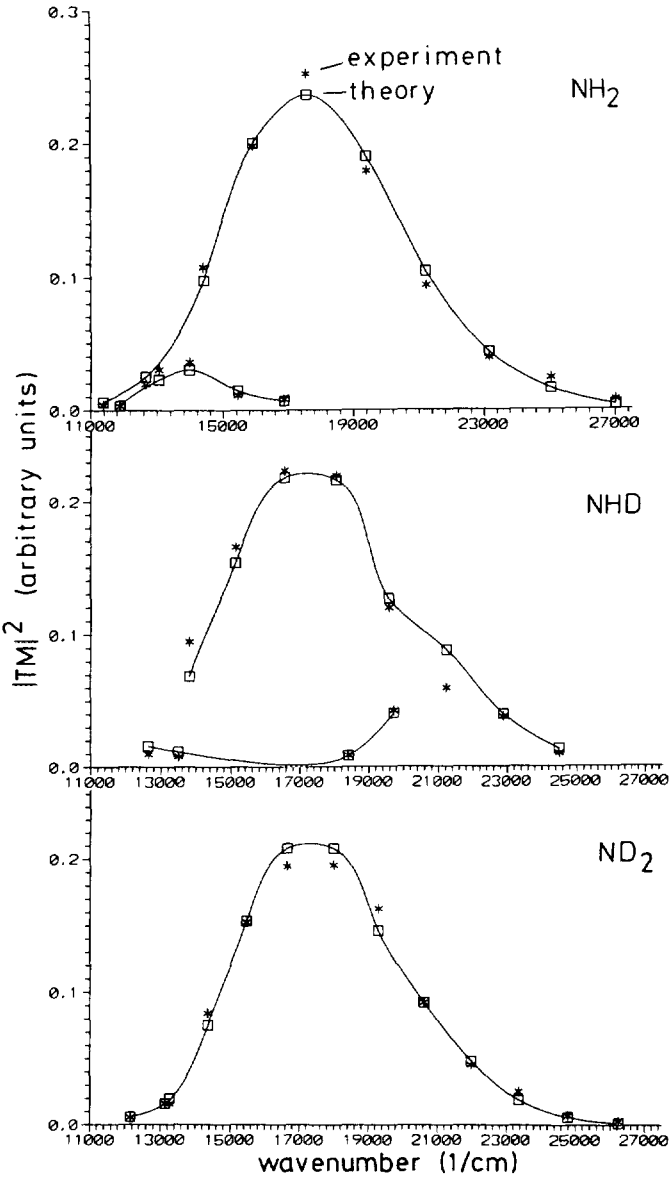

FIG. 7. Comparison of observed {*} with calculated {□} relative transition moments squared, $|TM|^2$, of NH_2, NHD, and ND_2.

our assignments. A notable exception is the 2+ II level splitting of ND_2 in solid argon, which is underpredicted by a factor of 3.

Transition Probabilities

The II bands in our low temperature spectra provide a valuable database for comparison with theoretically calculated relative vibronic transition moments squared $|TM|^2$, second columns in Tables II, IV, VII, and X, for $K'_a = 1 \leftarrow K''_a = 0$ transitions.

The complete Franck–Condon range of the $\tilde{A}\ ^2A_1 \leftarrow \tilde{X}\ ^2B_1$ transition, including transitions to Renner–Teller coupled levels of the $^2B_1$ state above the linearity barrier, is covered by our experimental data. Transition moments squared in relative units were deduced by numerically integrating the areas under the individual bands in the matrix: $|TM|^2 \propto \int \ln(I_0/I)d\nu/\nu_0$. The results for NH_2, NHD, and ND_2 in solid argon are compared with the theoretical data in Fig. 7. No systematic differences were noted between different rare gases within our relatively large error limits. The agreement between the experimental data $\{*\}$ and the theoretical calculations $\{\square\}$ is remarkable. A relatively large discrepancy between theory and experiment occurs for the 6+ band of NHD. This discrepancy is probably not significant in view of the fact that it is difficult to measure the true area of the weak 6+ absorption which is strongly overlapped by other absorptions. It should be noted that intensity borrowed from assigned as well as unassigned Fermi resonances was taken into account by summing over the band areas of resonant pairs. When the unassigned resonances were omitted from the band area determinations, the agreement between theory and experiment was less satisfactory.

5. SUMMARY

Absorption spectra of matrix-isolated NH_2 exhibit matrix shifts significantly below 0.5%, and linewidths of less than 5 cm^{-1}, in favorable cases less than 2 cm^{-1}, in Ne, Ar, Kr, and Xe matrices. Thus, spectra of NH_2, NHD, and ND_2 in Ar could be nearly completely assigned by comparison with term values from gas-phase studies and from theoretical calculations. Although the temperature dependencies of the spectra show that NH_2 and its deuterides behave like free rotors in the rare gas cage, forbidden $\Sigma^* \leftarrow \Sigma$ and $\Delta^* \leftarrow \Sigma$ transitions were identified, which become weakly allowed in rare gas matrices due to rotation–translation coupling with a local mode of ca. 70 cm^{-1}. Although the resolved spin splittings of the isotopomers deviate slightly from their gas-phase values, comparison with observed and calculated spin splittings has helped to prove or disprove assignments in the matrix spectra. The simplicity of the matrix spectra at low temperatures rendered possible several conclusive and some tentative assignments of resonances. Integrated band areas of II progressions in the low-temperature spectra, including Renner–Teller induced transitions to vibrational levels of the ground state above the barrier to linearity, compare very well with the square of theoretically obtained transition moments.

ACKNOWLEDGMENTS

This work was supported by Deutsche Forschungsgemeinschaft within Projects B3 and C3 of SFB 334. The work on relaxation of matrix-isolated NH_2 forms part of Project Schu 457/6-2.

RECEIVED: August 31, 1992

REFERENCES

1. K. DRESSLER AND D. A. RAMSAY, *Philos. Trans. R. Soc. London Ser. A* **25,** 553–602 (1959).
2. G. HERZBERG, "Molecular Spectra and Molecular Structure III. Electronic Spectra and Electronic Structure of Polyatomic Molecules," Van Nostrand–Reinhold, New York, 1966.
3. G. W. ROBINSON AND M. MCCARTY, *J. Chem. Phys.* **28,** 349–350 (1958).
4. G. W. ROBINSON AND M. MCCARTY, *J. Phys. Chem.* **30,** 999–1005 (1959).
5. D. E. MILLIGAN AND M. E. JACOX, *J. Chem. Phys.* **43,** 4487–4493 (1965).

6. M. KROLL, *J. Chem. Phys.* **63,** 319–325 (1963).
7. J. B. HALPERN, G. HANCOCK, M. LENZI, AND K. H. WELGE, *J. Chem. Phys.* **63,** 4808–4816 (1975).
8. V. M. DONNELLY, A. P. BARONAVSKI, AND J. R. MCDONALD, *Chem. Phys.* **43,** 283–293 (1979).
9. M. VERVLOET, *Mol. Phys.* **63,** 433–449 (1988).
10. S. C. ROSS, F. W. BIRSS, M. VERVLOET, AND D. A. RAMSAY, *J. Mol. Spectrosc.* **129,** 436–470 (1988).
11. CH. JUNGEN AND A. J. MERER, *Mol. Phys.* **40,** 1–23 (1980).
12. CH. JUNGEN, K.-E. J. HALLIN, AND A. J. MERER, *Mol. Phys.* **40,** 25–63 (1980).
13. CH. JUNGEN, K.-E. J. HALLIN, AND A. J. MERER, *Mol. Phys.* **40,** 65–94 (1980).
14. M. PERIĆ, S. D. PEYERIMHOFF, AND R. J. BUENKER, *Mol. Phys.* **49,** 379–400 (1983).
15. W. A. ANDERSON, *J. Phys. Chem.* **93,** 530–536 (1989).
16. D. A. RAMSAY AND F. D. WAYNE, *Can. J. Phys.* **57,** 761–766 (1979).
17. J. W. C. JOHNS, D. A. RAMSAY, AND S. C. ROSS, *Can. J. Phys.* **54,** 1804–1814 (1976).
18. R. D. KENNER, A. KAES, R. K. BROWARZIK, AND F. STUHL, *J. Chem. Phys.* **91,** 1440–1445 (1989).
19. R. J. BUENKER, M. PERIĆ, S. D. PEYERIMHOFF, AND R. MARIAN, *Mol. Phys.* **43,** 987–1014 (1981).
20. M. PERIĆ, R. J. BUENKER, AND S. D. PEYERIMHOFF, *Mol. Phys.* **59,** 1283–1303 (1986).
21. M. PERIĆ, S. D. PEYERIMHOFF, AND R. J. BUENKER, *Int. Rev. Phys. Chem.* **4,** 85–125 (1985).
22. J. T. HOUGEN, P. R. BUNKER, AND J. W. C. JOHNS, *J. Mol. Spectrosc.* **34,** 136–172 (1970).
23. P. R. BUNKER AND B. M. LANDSBERG, *J. Mol. Spectrosc.* **67,** 374–385 (1977).
24. S. CARTER AND N. C. HANDY, *Mol. Phys.* **52,** 1367–1391 (1984).
25. M. PERIĆ AND B. ENGELS, *J. Chem. Phys.* **97,** 4996–5006 (1992).
26. C. BLINDAUER, unpublished results.
27. CH. MARIAN AND R. KLOTZ, *Chem. Phys.* **95,** 213–223 (1985).
28. R. N. DIXON, ST. J. IRVING, J. R. NIGHTINGALE, AND M. VERVLOET, *J. Chem. Soc. Faraday Trans.* **87,** 2121–2133 (1991).
29. G. HERZBERG, "Molecular Spectra and Molecular Structure II. Infrared and Raman Spectra of Polyatomic Molecules," p. 215 ff, Van Nostrand-Reinhold, New York, 1945.
30. G. HERZBERG, "Molecular Spectra and Molecular Structure III. Electronic Spectra and Electronic Structure of Polyatomic Molecules." p. 151 f, Van Nostrand-Reinhold, New York, 1966.
31. A. RAMSTHALER-SOMMER, A. C. BECKER, N. VAN RIESENBECK, K.-P. LODEMANN, AND U. SCHURATH, *Chem. Phys.* **140,** 331–338 (1990).
32. C. BLINDAUER, N. VAN RIESENBECK, K. SERANSKI, M. WINTER, A. C. BECKER, AND U. SCHURATH, *Chem. Phys.* **150,** 93–108 (1991).
33. V. HIZHNYAKOV, K. SERANSKI, AND U. SCHURATH, *Chem. Phys.* **163,** 249–256 (1992).